Frascati Physics Series Vol. 72 (2022)
7TH YOUNG RESEARCHERS' WORKSHOP 'PHYSICS CHALLENGES IN THE LHC ERA'
July 11 and 14, 2022

ADDRESSING LEPTONIC $g-2$ ANOMALIES IN A FLAVOR CONSERVING TWO-HIGGS-DOUBLET MODEL

Carlos Miró
Departament de Física Teòrica and IFIC, Universitat de València-CSIC, E-46100, Burjassot, Spain
E-mail: Carlos.Miro@uv.es

Abstract

The discrepancy between the experimental determination of the muon and electron anomalous magnetic moments and their Standard Model expectations might be interpreted as New Physics. These anomalies can be addressed in the context of a general Flavor Conserving Two-Higgs-Doublet Model, which provides a simultaneous explanation in two regimes of scalar masses. The implications of the W boson mass measurement reported by the CDF Collaboration are also considered.

1 Introduction

Two anomalies related to the anomalous magnetic moment of leptons, $a_\ell = (g-2)_\ell/2$, have emerged. On the one hand, there exists a 4.2σ tension between the Standard Model (SM) prediction and the experimental determination of the muon anomalous magnetic moment reported by the Muon $g-2$ Collaboration [1],

$$\delta a_\mu^{\rm Exp} = a_\mu^{\rm Exp} - a_\mu^{\rm SM} = (2.5 \pm 0.6) \times 10^{-9}. \tag{1}$$

Despite the current discrepancies concerning the data-driven computation of the Hadronic Vacuum Polarization contribution and the latest results published by some lattice collaborations [2], we interpret this deviation as a sign of New Physics (NP). On the other hand, the electron anomalous magnetic moment might also be affected by NP. In this sense, depending on the input value of the fine structure constant determined from atomic recoils, a 2.4σ tension arises from ^{133}Cs measurements [3] and a 1.6σ tension from ^{87}Rb measurements [4]

$$\delta a_e^{\rm Exp,Cs} = -(8.7 \pm 3.6) \times 10^{-13}, \qquad \delta a_e^{\rm Exp,Rb} = (4.8 \pm 3.0) \times 10^{-13}. \tag{2}$$

A simultaneous explanation of these two anomalies has been considered in the context of general Flavor Conserving Two-Higgs-Doublet Models (2HDMs) [5, 6], that can also accommodate the recent CDF W boson anomaly [7].

In the following, we present the main features of the model in section 2. The new contributions to a_ℓ are addressed in section 3. Finally, we discuss our results in section 4 and summarize in section 5. For further details on this work, we refer to [6].

2 Model

The most general Yukawa sector in 2HDMs, assuming massless neutrinos, can be written as

$$\mathscr{L}_{\rm Y} = -\bar{Q}^0_L \left(Y_{d1}\Phi_1 + Y_{d2}\Phi_2\right) d^0_R - \bar{Q}^0_L \left(Y_{u1}\tilde{\Phi}_1 + Y_{u2}\tilde{\Phi}_2\right) u^0_R - \bar{L}^0_L \left(Y_{\ell 1}\Phi_1 + Y_{\ell 2}\Phi_2\right) \ell^0_R + \text{h.c.}, \qquad (3)$$

where Q^0_L and L^0_L are the SM left-handed quark and lepton doublets, respectively; d^0_R, u^0_R and ℓ^0_R, the SM right-handed quark and lepton singlets; Φ_1 and Φ_2, the two Higgs doublets, with $\tilde{\Phi}_j \equiv i\sigma_2\Phi^*_j$; and Y_{fi} ($f = d, u, \ell$ and $i = 1, 2$), the 3×3 Yukawa coupling matrices. All fermionic fields must be understood as 3-dimensional vectors in flavor space. It is convenient to rotate the scalar fields into the so-called *Higgs basis*, where only one scalar doublet acquires a vacuum expectation value (vev). Then, going to the fermion mass basis via the usual bidiagonalization procedure, it is straightforward to obtain

$$\mathscr{L}_{\rm Y} = -\frac{\sqrt{2}}{v}\bar{Q}_L \left(M_d H_1 + N_d H_2\right) d_R - \frac{\sqrt{2}}{v}\bar{Q}_L \left(M_u \tilde{H}_1 + N_u \tilde{H}_2\right) u_R - \frac{\sqrt{2}}{v}\bar{L}_L \left(M_\ell H_1 + N_\ell H_2\right) \ell_R + \text{h.c.}, \quad (4)$$

where the matrices M_f ($f = d, u, \ell$), coupled to the only Higgs doublet that acquires a vev, are the diagonal fermion mass matrices. However, the new flavor structures represented by the N_f matrices are not diagonal in general and thus can introduce dangerous Flavor Changing Neutral Currents. In order to avoid them, we consider a type I (or type X) quark sector, shaped by a $\mathbb{Z}_2$ symmetry, and a general Flavor Conserving (gFC) lepton sector, based on the hypothesis presented in [8]. Therefore,

$$N_d = t_\beta^{-1} M_d, \quad N_u = t_\beta^{-1} M_u, \quad N_\ell = \text{diag}(n_e, n_\mu, n_\tau), \qquad (5)$$

where $t_\beta \equiv \tan\beta = v_2/v_1$ is the ratio of the vevs of the scalar doublets in eq.3. The N_ℓ matrices in the lepton sector are diagonal, arbitrary and one loop stable under Renormalization Group Evolution (RGE) in the sense that they remain diagonal. The effective decoupling between muons and electrons arising from the independence of n_μ and n_e may allow us to explain both δa_ℓ anomalies within our I-gℓFC framework.

Completing the definition of the model, the scalar potential is built with the same $\mathbb{Z}_2$ symmetry, but it is softly broken by the term $\left(\mu^2_{12}\Phi^\dagger_1\Phi_2 + \text{h.c.}\right)$ with $\mu^2_{12} \neq 0$ in order to have scalar masses larger than 1 TeV and values of t_β larger than 8. Furthermore, we neglect CP violation in the scalar and the Yukawa sectors. In this way, our scalar spectrum contains two CP-even neutral scalars $\{\text{h}, \text{H}\}$, one CP-odd pseudoscalar A and two charged scalars $\text{H}^\pm$, with no mixing between the CP eigenstates. We will identify the state h with the 125 GeV scalar discovered at the LHC: this condition will lead to the so-called *scalar alignment limit* where the h couplings are SM-like. Finally, the new lepton Yukawa couplings are real, i.e., $\text{Im}(n_\ell) = 0$.

3 New Physics contributions to a_ℓ

The complete theoretical prediction for the anomalous magnetic moment of lepton ℓ consists of the sum of the SM prediction, $a_\ell^{\rm SM}$, and the NP correction, δa_ℓ:

$$a_\ell^{\rm Th} = a_\ell^{\rm SM} + \delta a_\ell. \tag{6}$$

One can factorize out the typical one loop factors and the SM Higgs-like couplings from the NP term as

$$\delta a_\ell = K_\ell \Delta_\ell, \quad K_\ell = \frac{1}{8\pi^2}\left(\frac{m_\ell}{v}\right)^2. \tag{7}$$

Aiming to solve the lepton anomalies, that is $\delta a_\ell = \delta a_\ell^{\rm Exp}$, one needs

$$\Delta_\mu \simeq 1, \quad \Delta_e^{\rm Cs} \simeq -16, \quad \Delta_e^{\rm Rb} \simeq 9. \tag{8}$$

On that respect, both one loop and two loop (of Barr-Zee type) diagrams can play a relevant role to explain the previous anomalies simultaneously. In the scalar alignment limit and keeping only leading terms in a m_ℓ^2/m_S^2 ($S = {\rm H}, {\rm A}, {\rm H}^\pm$) expansion, the one loop result reads

$$\Delta_\ell^{(1)} \simeq |n_\ell|^2 \left(\frac{I_{\ell {\rm H}}}{m_{\rm H}^2} - \frac{I_{\ell {\rm A}} - 2/3}{m_{\rm A}^2} - \frac{1}{6 m_{{\rm H}^\pm}^2} \right), \tag{9}$$

where

$$I_{\ell S} = -\frac{7}{6} - 2\ln\left(\frac{m_\ell}{m_S}\right). \tag{10}$$

Under the same assumptions, the two loop contribution is given by

$$\Delta_\ell^{(2)} \simeq -\frac{2\alpha}{\pi}\frac{{\rm Re}(n_\ell)}{m_\ell} F, \tag{11}$$

where

$$F = \frac{t_\beta^{-1}}{3}\left[4(f_{t{\rm H}} + g_{t{\rm A}}) + (f_{b{\rm H}} - g_{b{\rm A}})\right] + \frac{{\rm Re}(n_\tau)}{m_\tau}(f_{\tau {\rm H}} - g_{\tau {\rm A}}), \tag{12}$$

with $f_{fS} = f(m_f^2/m_S^2)$ and $g_{fS} = g(m_f^2/m_S^2)$ depending only on the scalar and fermion masses, as defined in [6]. In the following section, we explore how to solve the lepton anomalies through these new contributions.

4 Analysis and results

The aim of this work is to identify which regions of the parameter space of the model are able to reproduce the δa_ℓ anomalies while satisfying all relevant low and high energy constraints. The list of constraints, modelled with a gaussian likelihood factor or an equivalent χ^2 term, reads as follows (for details, see [6]).

- Perturbative unitarity of $2 \to 2$ high energy scattering of scalars, perturbativity of the quartic couplings in the scalar potential [9] and boundedness from below [10].
- Signal strengths of the 125 GeV Higgs boson [11, 12, 13, 14, 15, 16, 17, 18, 19, 20, 21, 22, 23] that we identify with the CP-even state h: this condition forces the alignment limit in the scalar sector.

- Agreement with electroweak precision data through corrections in the oblique parameters S and T [24, 25], that requires near degeneracies $m_{\mathrm{H}^\pm} \simeq m_{\mathrm{H}}$ and/or $m_{\mathrm{H}^\pm} \simeq m_{\mathrm{A}}$ in the scalar spectrum.
- LEP data from $e^+e^- \to \mu^+\mu^-, \tau^+\tau^-$ with center-of-mass energies up to $\sqrt{s} = 208$ GeV [26]: this constraint essentially imposes $m_{\mathrm{H}}, m_{\mathrm{A}} > 208$ GeV.
- LHC direct searches of new scalars: resonant processes $pp \to S \to \mu^+\mu^-, \tau^+\tau^-$ ($S = \mathrm{H}, \mathrm{A}$) via gluon-gluon fusion [27, 28, 29, 30, 31] and $\mathrm{H}^\pm$ searches in $pp \to \mathrm{H}^\pm tb$, $\mathrm{H}^\pm \to \tau\nu, tb$ [32, 33, 34, 35].
- $\mathrm{H}^\pm$-induced processes that must be kept under control in Lepton Flavor Universality (LFU) measurements concerning purely leptonic decays $\ell_j \to \ell_k \nu\bar{\nu}$ as well as pseudoscalar meson decays $K, \pi \to e\nu, \mu\nu$ [24, 36, 37], and in $b \to s\gamma$ and $B_q^0 - \bar{B}_q^0$ mixing processes [24, 38, 39].
- Perturbativity upper bounds on the new lepton Yukawa couplings, namely $|n_\ell| \leq 250$ GeV.

In the plots below, we show selected results of the allowed parameter space of the model where $\delta a_\mu^{\mathrm{Exp}}$ and $\delta a_e^{\mathrm{Exp,Cs}}$ are solved (other scenarios concerning δa_e will be treated in the following section). The different colors represent three contours in the joint $\Delta\chi^2 = \chi^2 - \chi^2_{\mathrm{Min}}$. In a 2D-$\Delta\chi^2$ distribution they correspond, darker to lighter, to 1, 2 and 3σ regions.

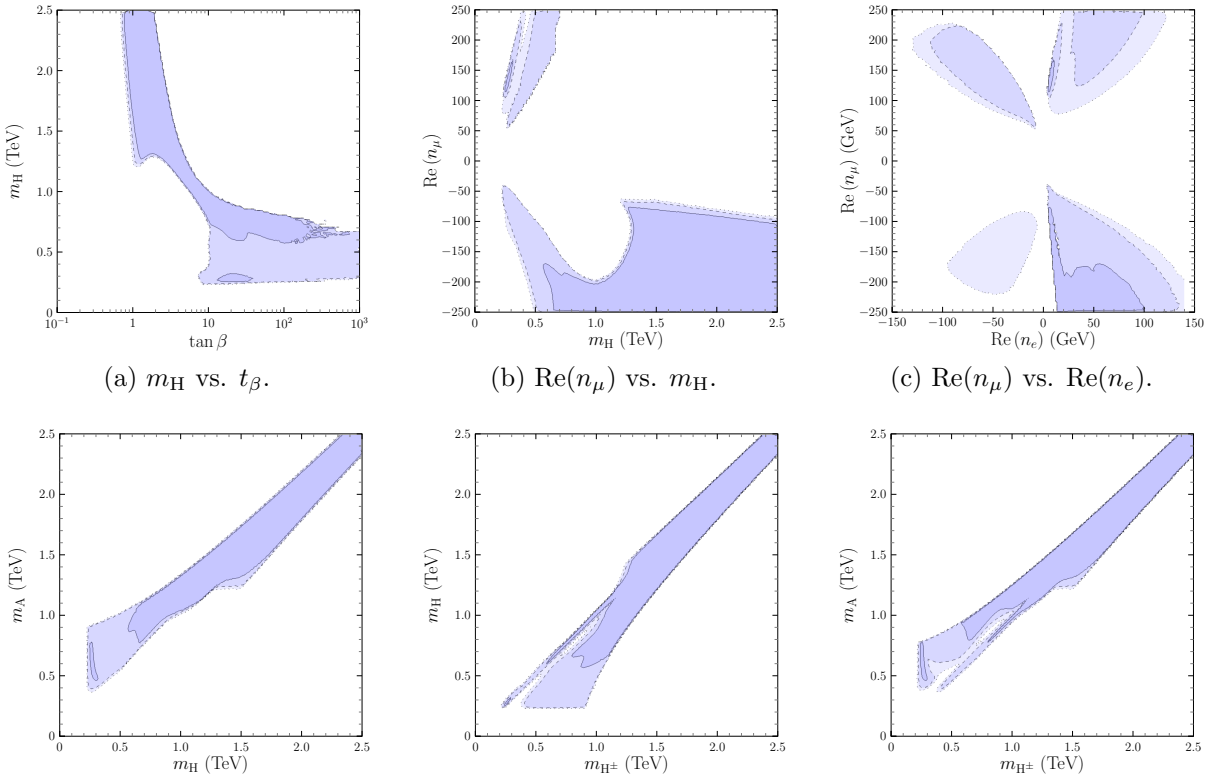

(a) m_{H} vs. t_β. (b) $\mathrm{Re}(n_\mu)$ vs. m_{H}. (c) $\mathrm{Re}(n_\mu)$ vs. $\mathrm{Re}(n_e)$.

(d) m_{A} vs. m_{H}. (e) m_{H} vs. $m_{\mathrm{H}^\pm}$. (f) m_{A} vs. $m_{\mathrm{H}^\pm}$.

Figure 1: *Illustrative plots of the allowed parameter space where the δa_ℓ anomalies are reproduced.*

In fig.1a one can roughly distinguish two types of solutions: (i) all scalar masses above 1.2 TeV and the ratio of the two vevs $t_\beta \sim 1$, and (ii) all new scalars masses in the [0.2;1.2] TeV range and $t_\beta > 10$.

In the low mass solution, the muon anomaly is explained at one loop through the H contribution and thus $\mathrm{Re}(n_\mu)$ can appear with both signs, as fig.1b illustrates. Instead, for heavy new scalars, the muon anomaly receives dominant two loop contributions in such a way that the muon coupling is fixed to be negative. On the other hand, the electron anomaly must be explained at two loops in the whole range of scalar masses when considering the previous constraints. In particular, the latter implies the existence of a linear relation between both lepton couplings given by $\mathrm{Re}(n_\mu) \simeq -13\mathrm{Re}(n_e)$, as can be seen in the lower part of fig.1c inside the darkest region: departure from this straight line introduces an important one loop contribution to the muon anomaly lowering also the scalar mass ranges. Finally, from figs.1d–1f, it is easy to check that all new scalars are degenerate in the heavy mass regime, with mass differences not exceeding 200 GeV; while, in the low mass region, the pseudoscalar is heavier than the scalar and the charged scalar is degenerate with either the scalar or the pseudoscalar.

4.1 Different scenarios for δa_e

So far we have focused on the value of the electron anomaly related to the Cs recoil measurements of the fine structure constant. This scenario is more challenging from the theoretical point of view due to the opposite sign of both leptonic anomalies. Nevertheless, in order to have a complete picture, we have performed the analyses taking into account the Rb case and also an average scenario combining these two results, namely $\delta a_e^{\mathrm{Exp,Avg}} = -(2.0\pm2.2)\times10^{-13}$. Although $\delta a_e^{\mathrm{Exp,Cs}}$ and $\delta a_e^{\mathrm{Exp,Rb}}$ are rather incompatible, this average value might be interesting to analyze since it has also negative sign, i.e. opposite to the muon anomaly, but it is roughly 4 times smaller than the Cs value.

The final results show that the main difference among the analyses is the change of sign of the electron coupling depending on the case, as can be checked in fig.2. There are also changes concerning the extension of the allowed regions, but the main features of our solutions still apply.

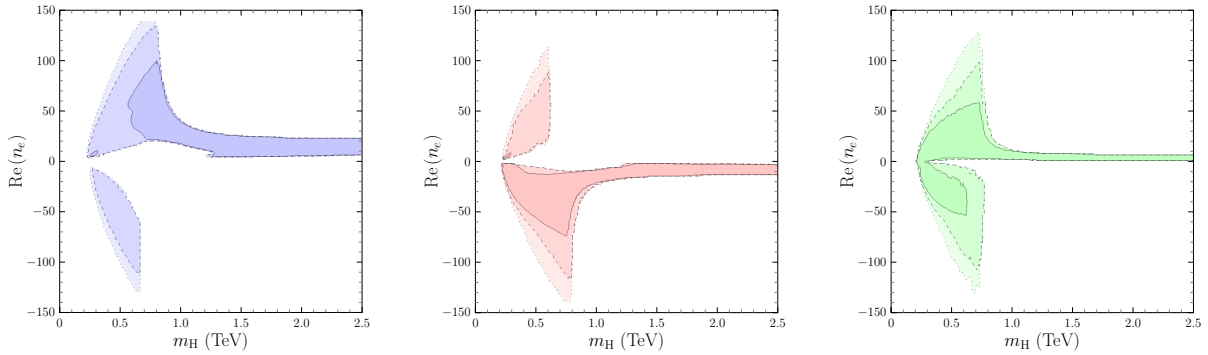

(a) $\delta a_e^{\mathrm{Exp,Cs}}$. (b) $\delta a_e^{\mathrm{Exp,Rb}}$. (c) $\delta a_e^{\mathrm{Exp,Avg}}$.

Figure 2: $\mathrm{Re}(n_e)$ *vs.* m_{H} *in the different scenarios considered for* $\delta a_e^{\mathrm{Exp}}$.

4.2 The CDF W boson mass anomaly

The recent measurement of the W boson mass reported by the CDF Collaboration [7] can also be addressed in this framework through deviations in the oblique parameters $(\Delta S, \Delta T) \neq (0, 0)$. In particular, we consider two scenarios: (i) a "conservative" average between the CDF value and previous measurements

of the W mass, and (ii) only using the CDF result. In this section, the analyses are performed using the value of the electron anomaly arising from Cs recoil, that is, $\delta a_e^{\rm Exp,Cs}$.

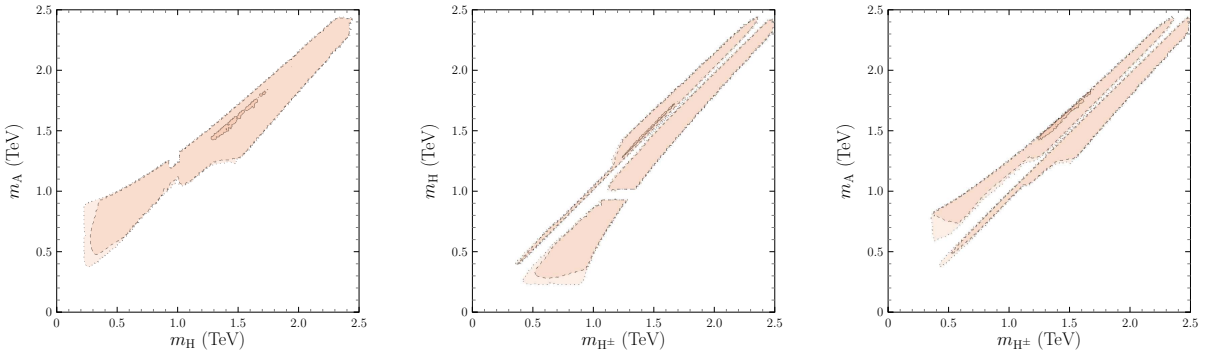

(a) $m_{\rm A}$ vs. $m_{\rm H}$. (b) $m_{\rm H}$ vs. $m_{\rm H^\pm}$. (c) $m_{\rm A}$ vs. $m_{\rm H^\pm}$.

Figure 3: *Correlations involving the scalar masses in the "conservative" average scenario.*

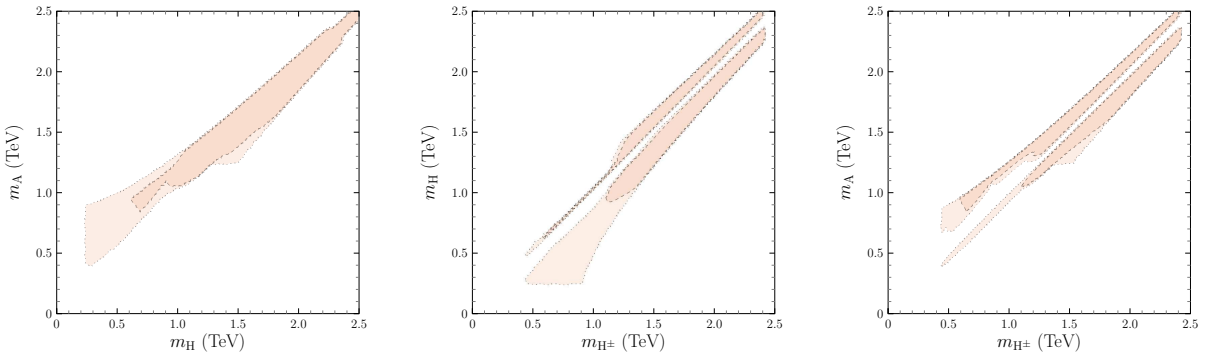

(a) $m_{\rm A}$ vs. $m_{\rm H}$. (b) $m_{\rm H}$ vs. $m_{\rm H^\pm}$. (c) $m_{\rm A}$ vs. $m_{\rm H^\pm}$.

Figure 4: *Correlations involving the scalar masses in the scenario that only uses the CDF result.*

Figs.3 and 4 show the correlations among the scalar masses in these two scenarios. As one can easily check, scalar masses larger than 2 TeV are more difficult to obtain and near degeneracies $m_{\rm H^\pm} \simeq m_{\rm H}$ and $m_{\rm H^\pm} \simeq m_{\rm H}$ are absent. In fact, overall agreement with the previous constraints is worse in several regions of the parameter space, specially in the second scenario. Despite these changes, the main features of our solutions, previously mentioned, remain unchanged.

5 Summary

We present a particular Two-Higgs-Doublet Model, type I (or X) in the quark sector and general Flavor Conserving in the lepton sector, that is stable under one loop RGE and allows for LFU violation beyond the mass proportionality. This framework provides a simultaneous explanation of both $(g-2)_{\mu,e}$ anomalies in two possible regimes: (i) scalar masses in the [0.2;1.2] TeV range with $t_\beta \gg 1$, or (ii) scalar masses above 1.2 TeV and $t_\beta \sim 1$. The electron anomaly is explained through two loop Barr-Zee contributions in the whole range of scalar masses, while the muon anomaly also receives important one loop contributions

in the low mass region. Different assumptions concerning the value of the electron anomaly are fully considered. Furthermore, the CDF W boson anomaly can also be accommodated in this context.

Acknowledgements

CM is funded by *Conselleria de Innovación, Universidades, Ciencia y Sociedad Digital* from *Generalitat Valenciana* under grant ACIF/2021/284. CM acknowledges the organizers of the XX LNF Summer School 'Bruno Touschek' for the opportunity to present this work.

References

1. Muon $g-2$ Collaboration, Phys. Rev. Lett. **126**, 14 (2021).
2. S. Borsanyi *et al*, Nature **593**, 51 (2021).
3. R.H. Parker *et al*, Science **360**, 191 (2018).
4. L. Morel *et al*, Nature **588**, 61 (2020).
5. F.J. Botella *et al*, Phys. Rev. D **102**, 3 (2020).
6. F.J. Botella *et al*, arXiv:2205.01115.
7. CDF Collaboration, Science **376**, 170 (2022).
8. F.J. Botella *et al*, Phys. Rev. D **98**, 3 (2018).
9. I.F. Ginzburg *et al*, Phys. Rev. D **72**, 11 (2005).
10. I.P. Ivanov *et al*, Phys. Rev. D **92**, 5 (2015).
11. ATLAS Collaboration, Eur. Phys. J. C **81**, 6 (2021).
12. ATLAS Collaboration, Eur. Phys. J. C **81**, 2 (2021).
13. ATLAS Collaboration, ATLAS-CONF-2020-058 (2020).
14. ATLAS Collaboration, ATLAS-CONF-2020-026 (2020).
15. ATLAS Collaboration, Phys. Lett. B **812**, (2021).
16. ATLAS Collaboration, ATLAS-CONF-2020-027 (2020).
17. ATLAS Collaboration, Phys. Lett. B **798**, (2019).
18. ATLAS Collaboration, Eur. Phys. J. C **80**, 10 (2020). [Erratum: Eur. Phys. J. C **81**, 29 (2021), Eur. Phys. J. C **81**, 398 (2021)].
19. CMS Collaboration, CMS-PAS-HIG-16-003 (2016).
20. CMS Collaboration, CMS-PAS-HIG-19-005 (2020).
21. CMS Collaboration, JHEP **01**, 148 (2021).
22. CMS Collaboration, JHEP **07**, 027 (2021).

23. CMS Collaboration, Eur. Phys. J. C **81**, 6 (2021).

24. P.A. Zyla *et al*, Review of Particle Physics, PTEP **2020**, 8 (2020).

25. W. Grimus *et al*, Nucl. Phys. B **801**, 81 (2008).

26. ALEPH Collaboration, Eur. Phys. J. C **49**, 411 (2007).

27. ATLAS Collaboration, JHEP **10**, 182 (2017).

28. CMS Collaboration, Phys. Lett. B **798**, (2019).

29. ATLAS Collaboration, JHEP **01**, 055 (2018).

30. CMS Collaboration, JHEP **02**, 048 (2017).

31. CMS Collaboration, JHEP **09**, 007 (2018).

32. ATLAS Collaboration, JHEP **11**, 085 (2018).

33. CMS Collaboration, JHEP **07**, 142 (2019).

34. CMS Collaboration, JHEP **01**, 096 (2020).

35. CMS Collaboration, JHEP **07**, 126 (2020).

36. V. Cirigliano *et al*, Phys. Rev. Lett. **99**, 23 (2007).

37. A. Pich *et al*, Prog. Part. Nucl. Phys. **75**, 41 (2014).

38. M. Misiak *et al*, Phys. Rev. Lett. **98**, 2 (2007).

39. A. Crivellin *et al*, Phys. Rev. D **87**, 9 (2013).